The Caucasus Territory Hot-Cold Spots Determination And Description Using 2D Surface Waves Tomography

Seyed Hossein Abrehdari (abrehdari@ut.ac.ir)
National Academy of Science
Jon K. Karapetyan
National Academy of Science
Habib Rahimi
University of Tehran
Eduard Gyodakyan
National Academy of Science

Research Article

Keywords: Caucasus territory, Hot-Cold spots determination, 2D surface wave tomography, Geothermal resources, Single-Station method

Posted Date: December 20th, 2021

DOI: https://doi.org/10.21203/rs.3.rs-700822/v2

Abstract

In order to identify and describe Hot-Cold spots inside the earth based on increasing and decreasing wave velocity anomalies, this paper attempts to generate the first 2D tomographic maps of Rayleigh surface wave velocity dispersion curves, by using ~1200 local-regional earthquake data and ~30000 vertical (Z) components of earthquake data waveform energy with magnitude M≥4 from 1999 to 2018 in a periods range of 5 to 70 seconds and a grid spacing of 0.2º×0.5º for a depth of ~200 km. To conduct this, a generalized 2D linear inversion procedure developed by Yanovskaya and Ditmar has been applied to construct the first 2D Rayleigh tomography velocity maps in order to understand better the regional tectonic activities in the enigmatic ongoing collision-compressed edge zone of the Eurasian-Arabic plates. In this study, we assumed that low-velocity (slow) region with dark red shade is hot spot and high-velocity (fast) region with dark blue-green-yellow is a cold spot. In short and medium periods were determined the number of 15 and 2 hot spots with a depth of 7 to 108 km, respectively. In long-periods and a depth of ~200 km, most part of the area study has covered by low-velocity anomaly.

1. Introduction

Many questions have been raised about the thermal and mechanical development of faults movement, passive margins based on the effects of plates-boundary interactions, lithospheric processes and mantle activity, in addition to continental thinning and generally the heat beneath our feet. The earthquakes waves are originating in Earth’s crust or upper mantle, which ricochet around the earth’s interior and traveling most rapidly through cold, dense regions and more slowly through hotter rocks. The geologists to map earth’s interior, use the seismic waves chart movement (traces) generated by earthquakes that has been recorded by a worldwide network of seismometers. Each recorded wave trace reveals many useful informations from the extent and density of Earth’s deepest regions. According to the seismic tomography images of Suzan van der Lee and Steve Grand (2019) studies (also visit this website: [https://www.iris.edu/hq/inclass/fact-sheet/seismic_tomography]) from within the earth, the colors show anomalies in rigidity, which correlate with temperature anomalies. The dark blue-green-yellow shades mean colder and stiffer rock (cold spots) that are the remnants of an old tectonic plate that has been subducted underneath the Earth plates (large cold and aseismic area during million years) and dark red shades mean warmer and weaker regions (hot spots). Geologists believe that a hot spot is a location on the Earth's surface that has experienced active volcanism for a long period of time and the places known as hot spots or temples are volcanic regions thought to be fed by underlying mantle that is anomalously hot compared with the surrounding mantle. The origins of the concept of hot spots lie in the work of Wilson, J. Tuzo (1963), who postulated that the formation of the hot spot is from the slow movement of a tectonic plate across a hot region beneath the surface. It was later postulated that hot spots are fed by columns or narrow streams of magma or hot mantle rising from the Earth's core-mantle boundary in a structure called a mantle plume, which hot spot develops above the plume. Magma generated by the hot spot rises through the rigid plates of the lithosphere and produces active volcanoes at the Earth's surface. Geologists have identified some 40-50 such hot spots around the globe, which Hawaii, Reunion,

Yellowstone, Galapagos and Iceland overlying the most currently active (supplementary file, Fig. S1). However, keep in mind these are just theories and nobody really knows the answer. The honest answer is that lots of folks are working on it but haven't come up with the answer yet.

Hot spots (close to the earth's surface) are the same geothermal resources that exists in the Earth's solid crust through a mantle plume (the deep part of the earth) and is useful for identifying sources of geothermal energy. Unlike other renewable energies, geothermal energy is not limited to specific seasons, times and conditions, it can be exploited without interruption, and it is even much cheaper than other types of new energies. For example, countries such as Iceland (Nesjavellir Geothermal Power Plant), New Zealand (Wairakei Geothermal Power Plant), Turkey (Gürmat 2 Geothermal Power Plant) and NW Iran (using water from hot springs or hydrothermal) use this energy. In effect of the chemical interactions, volcanic zones, tectonic activities, high temperatures and pressures in the earth's interior some of the rocks melted, the solid behavior becomes plastically and geothermal zones (hot spots) arise. This paper attempts to generate the first 2D tomographic inversion of Rayleigh wave dispersion maps in order to identify and describe Hot-Cold spots inside the earth based on *fast* and *slow* wave velocity anomalies. These maps show excellent agreement with results of previous studies and many of the geological features of the Caucasus territory. In order to understand better and study hot-cold spots, can be mentioned to some studies like Suzan van der Lee et al. (2019), and Michael Wysession (2010-2020). Also, the website [https://en.wikipedia.org/wiki/Hotspot_(geology)] and its 25 related references are very useful. The Rayleigh wave group velocity dispersion curves for each source-station path are estimated using the do_ mft command of Hermann's software. Then, using a 2D-linear inversion method developed by Ditmar and Yanovskaya (1987) and Yanovskaya and Ditmar (1990), the 2D group velocity maps are generated. Some studies of the crustal structure have been conducted related to the estimation of the crustal thickness beneath this region (e.g. NW Iran: Gheitanchi, 1996; EAAC: Skobeltsyn, G. et al., 2014; Caucasus: Randolph J. Martin et al., 2007). As well as, this study benefits from new permanent seismic stations installed in Turkey, Azerbaijan, Georgia, Armenia and NW Iran, which provides much better rays path coverage in the Caucasus for the resolution of tomographic images.

2. Caucasus General Information And Pervious Studies

The structure of the Caucasus mountain region and surrounding areas is primarily controlled by the collision and continuing convergence of the Arabian and Eurasian plates. Over time, this motion led to subsequent collision stages between Arabia and smaller continental blocks resulted from the break-up of Gondwana until the final closure of Neo-Tethys Ocean. Because of this geodynamic evolution, a complex geological structure has formed that characterized by important lateral variations in age, composition and tectonic style (Hatzfeld and Molnar, 2010). Greater Caucasus (GC), Lesser Caucasus (LC), East Anatolian Accretionary Complex (EAAC), Bitlis Massif (BM), Pontide (PN), NW Iran, Tlesh (TAL), South Caspian Basin (SCB), Kura Basin (KB), Rioni Basin (RB) and Eastern Blake Sea Basin (EBSB) are some part of the Arabia-Eurasia collision (Figs. 1 and 2). The Greater Caucasus mountains are an orogenic belt that was raised as a result of the collision, with altitudes of more than 5 km above sea level and 1,300 km

in the NW-SE direction between the Black Sea and the southern basin of the Caspian Sea. The convergence between Arabia and Eurasia began in Late Cretaceous (Golonka, 2004).

According to some studies (e.g. Copley and Jackson, 2006; Jackson, 1992; Randolph J. Martin, 2007; Talebian and Jackson, 2002) this continent-continent collisional tectonics processes has begun at about 12 Ma. Caucasus region is compressed between Arabian-Eurasian plates and due to N-S compression expanded the main seismo-active structures in NW Iran, Greater Caucasus (GC), Lesser Caucasus (LC), Eastern Anatolian Accretionary Complex (EAAC). The fault zones include reverse strike-slip, strike-slip sinistral, strike-slip dextral, wrench and major thrust faults with WNW-ESE direction are developed; and also the extensional axes with N-S direction relative movement of the Arabian plate against the Eurasian plate are formed (Figs. 1 and 2). Further, several large Neogene-Quaternary strato-volcanoes (<0.4 Ma- 6.5 Ma; Bavali et al., 2016) such as Elbrus is located in this region. Estimates of the overall N-S shortening across both the Greater and Lesser Caucasus are approximately 10+/-2 mm/yr of which ~60% is accommodated by the greater Caucasus. These studies indicate, however, that there is little internal shortening within the Greater Caucasus and that the present rate of shortening across the Caucasus cannot account for all the observed strain in the region (McClusky et al., 2000). According to some studies (e.g. Sosson et al., 1977; Alik Ismail-Zadeh et al., 2020), the Caucasus ranges incload the Greater Caucasus, is consisting mostly of Paleozoic metasedimentary rocks and granitoids, Jurassic sediments, Mesozoic and Cenozoic volcanism and the Lesser Caucasus consist Paleozoic granitoid metamorphic basement overlain unconformably by shelf carbonates of Paleozoic Triassic age, respectively. In this enigmatic area, there are complicated geological structures and large volcanic complexes and basins. As it is seen in Fig. 1, main magmatic arcs are responsible of the several large earthquakes in the Caucasus. Therefore, the arcs can be considered as a hot structure with high tectonic activities and interactions. In this study in addition to determining hot and cold spots, was investigated the structure of the crust and the uppermost mantle for Caucasus using surface wave tomography. To do this, we use the local-regional earthquake data recorded by the 47 broadband stations (table S1) and the results are presented for the periods 5 to70 s. Our results for the lower periods show distinct velocity anomalies along the Caucasus faults, magmatic arcs, basins and beneath the volcanoes. The results for the longest period (the uppermost mantle) show low-velocity anomalies for most parts of the study area. Regarding the study of Caucasus tomography, it should be noted that this method has not previously been used in the Caucasus area and its advantage is that it works in areas without uniformly coverage of rays. The velocity values are computed as an average of values given along the rays. The results are consistent with major geological and tectonic structures and the previous studies as well. However, the existence of a denser network of stations could be helpful in determining small-scale anomalies.

3. Method, Data And Measurements

3.1. Method: Two-dimensional tomography

Waves travel faster through cold-rigid material (like a subduction plate inside the mantle) and pass through warmer materials more slowly (like hot rocks rising to the surface). Seismic tomography is like

taking a Computed Tomography or CAT scan of the Earth. In a method similar to CT scans, scientists instead use seismic waves to make images of Earth's interior. When the ground shakes at the start of an earthquake, seismic waves race outwards from it (Kinahan P, Townsend D., 1998). In other words, the earthquakes waves are originating in Earth's crust or upper mantle, which ricochet around the earth interior and traveling most rapidly through cold, dense regions and more slowly through hotter rocks. In this study, a 2D-linear inversion method developed by Ditmar and Yanovskaya (1987) and Yanovskaya and Ditmar (1990) has been used to generate the group velocity maps. This method is a generalization of the classical 1-D method of Backus and Gilbert (1968). *When the averaging area parameter is used in the tomography study, there is no need for a checkerboard test.* The tomographic method estimates a group velocity map V(x) at each period by minimizing the following misfit function (Lihua Fang et al., 2008):

$(d - Gm)^T(d - Gm) + \iint$

1

Where

m\left(x,y\right)={{(V}^{-1}}_{(x,y)}-\left({V}_{0}^{-1}\right){\text{V}}_{0}

2

Where

{d}_{i}={t}_{i}- {t}_{i0}

3

{\left(\text{G}\text{m}\right)}_{i} =\iint {\text{G}}_{i}\left(x\right)dx= \underset{{l}_{oi}}{\overset{}{\int }}m\left(x\right)\frac{ds}{{\text{V}}_{0}}

4

\iint {\text{G}}_{i}\left(x\right)dx= \underset{{l}_{oi}}{\overset{}{\int }}\frac{ds}{{\text{V}}_{0}}= {\text{t}}_{i0}

5

The α-parameter controls the trade-off between the fit to the data and the smoothness of the resulting group velocity maps. Therefore, to improve the resolution and having a real model, we tested various values of the regularization parameter. Finally, we chose α = 0.2 that gives relatively smooth maps with small solution errors that this was conducted by testing different α values and observing the number of rays passing through each cell 0.2° × 0.5° (20 × 50 km^2). We waiver the perfect discussion about estimation of lateral resolution using the averaging area (*L*) and stretching \left(ex or {\epsilon }\right) parameters due to the elongation of the subject. The table S2 and Fig. S5 shows the changes in stretching, data density and averaging area parameters for some different periods. Large values of this parameter ex or {\epsilon } > 1 imply that the paths have a certain orientation and along these directions the resolution will probably be very small. In our study, L = 1232.215 and ex or ε =0.6985≅ 0.7) was obtained.

3.2. Data and measurements

The study area is located between 38°- 53° degrees east and 37°- 44° degrees north (Fig. 2). In this study, as mentioned; single-station method was used and a total of ~1200 local-regional events with magnitude

(M\ge 4), recorded by the 47 broadband and short-period stations in Seismic Network Incorporated Research Institutions for Seismology (IRIS) stations, including Armenia (GNI), Georgia (GO), Turkey) (TK, TU) and Azerbaijan (AB) were used as the primary database during the period 1999 to 2018. Earthquake data recorded by the Iranian Seismological Center-Tabriz Network and International Institute of Earthquake Engineering and Seismology (IIEES) are also have been used (Table S1). Figure S2. a) shows seismic stations used in this study, b) number of raypaths in each period, and c) Raypaths coverage map used in the tomographic inversion. After preliminary correction, for each station-earthquake pair, the frequency-time analysis of surface waves was used to estimate the dispersion curves. In processing with using 2D-linear inversion method developed by Ditmar and Yanovskaya (1987) and Yanovskaya and Ditmar (1990) to estimate group velocity dispersion curves, we have used Multiple Filter Technique (MFT) and Time Variable Technique (TVF) to separate the fundamental mode of approximately 30000 vertical (Z) components of surface waves motion of earthquake data waveform energy (Fig. S3). For this purpose, first, the fundamental mode of the Rayleigh surface waves group velocity dispersion curves was separated using the do_mft command of Hermann's software (Herrmann, R. B., Ammon, C. J., 2004) for different source-station paths. Then, by using GSAC, GMT software and computer specialized cods in Ubuntu operating system and MATLAB software, 2D tomography group velocity, stretching area, data density and averaging area maps were plotted and estimated for periods of 5-70 seconds. This method is used for estimating phase and group velocity of surface waves. It passed the preprocessed signal through a system of narrow-band filters in which the central frequency is varying. Besides, the amplitude of filter outputs is visualized in time and frequency domains. Then, on the Hermann diagram, the group velocity dispersion curve for each path is obtained. Fig. S3a) shows the raw seismograph and the cleaned waveform. Fig. S3b) shows the dispersion curve measurement by do_mft command of Hermann’s software to separate the fundamental mode of earthquake data waveform energy and Fig. S3c) shows an example of dispersion curve of cleaned waveform, for an earthquake recorded in the GNI (Garni station, Armenia). In fact, the high-energy red zone (top) is related to cleaned waveform of seismogram trace-vertical (Z) component. Since estimating the dispersion curves depends on magnitude, epicenteral distance, depth, etc., so different period ranges by applying do_mft command to every epicenter-station pair are obtained, hence for different periods we have various path numbers. The average distance between all epicenter-station paths is of the order of 500 km.

The resolution of the group velocity maps depends mostly on the density of paths and their azimuthal distribution (crossing paths). In our case, these two parameters depend on the geometry of the seismic array and on the distribution of the earthquakes that can limit the number of available paths for some directions. Finally, a set of dispersion curves were estimated for the fundamental mode Rayleigh wave in the period range from 5 to 70 s.

4. Results And Discussion

4.1. Hot-Cold spots determination and description using tomography velocity maps

As mentioned earlier, according to wave studies from within the earth, the earthquakes waves are originating in Earth's crust or upper mantle, which traveling most rapidly through cold, dense regions, and more slowly through hotter rocks. *Thus, in this study, we assumed that each low-velocity (slow) region with a dark red shade is a hot spot and each high-velocity (fast) region with dark blue-green-yellow shade is a cold spot.* So, in order to identify and describe Hot-Cold spots inside the earth based on increasing and decreasing wave velocity anomalies, the obtained 2D tomographic velocity maps in Fig. S4 and Fig. 3 shows this property. Schematic diagram of Fig. S7 in Supplementary Materials, has depicted to understand better the hot-cold spots procedure inside the earths. It shows the physical processes within the Earth's upper mantle that lead to the generation of magma in steps A to D for different plate tectonic settings. Tomographic maps with distinct velocities over short-periods of 5 to 25 seconds (equivalent to a depth of 6 to 53 km), are more sensitive to the structure of the upper to lower crust, and Moho. These periods represent sediments in the basins, chemical interactions of hydrocarbon resources, molten material and magma chambers beneath volcanoes and Moho discontinuity which these areas can be considered temporary and unstable hot and cold spots. These short-periods, which is also known as the crust, include soil, vegetation growth, construction, surface-groundwater, oil-gas resources, magma chambers, metallic, non-metallic mines, and chemical interactions. Although, slow velocities in crust/upper mantle under regions of active volcanism do not require "Hot Spot" (i.e, plume-related) magmatism. These could simply reflect decompression melting and/or crustal melting following slab-rollback, delamination, or breakoff. The lithosphere-aesthenosphere and upper mantle is the source of volcanic lava and the origin of some earthquakes in the mantle and remnants of the old tectonic plate. So, short-periods of 5 to 25 seconds can be considered temporary and unstable hot and cold spots. Dark red spots that are seen below the chain of volcanoes (e.g. Elbrus), upon some segments of faults, and basins in the study area indicate the hot spots and these hot spots, are located in an appropriate depth of shallow area of the earth's crust as geothermal energy resources. The rest of the areas on the tomography maps with various periods that has shown with shades dark blue-green-yellow, include colder and more rigid rocks and stones and remnants of an old tectonic plate and is calm (aseismic), which represent cold spot. Cold spots usually cover a wide area and can even cover tectonic plates and continents and even can include the mantle-core, which the mantle is the source of cold (old) lava volcanic and some deep earthquakes. The core is the Earth planet balance in the solar system and its magnetic property.

Dark red Low-velocity area which we assume as a hot spot **number 1**; there are 8 hot spots in period of 5 seconds that hot spot number 1 in our study (Fig. 3), there is a small area near Kars mountain in NE Turkey (Eastern Anatolia) known as the Erzurum-Kars Volcanic Plateau (EKVP)- (with depth ~6.6 to 13.33 km). According to Duru Olgun et al., (2020) study, this part of the plateau is known to have been formed by the eruptions during the Zanclean (~4.5 Ma) period, related an earlier continental collision event between Eurasian and Arabian continents ~15 Ma ago. Also, Eastern Anatolia is known for its thin lithosphere (Sengör, A. M. C. et al., 2003). The EKVP is composed mainly of andesitic and dacitic lavas and their trachytic equivalents intercalated with acidic ignimbrites and tuffs. In the northwest of Kars, an eroded stratovolcano is present which is possibly coeval with the plateau. It consists of a thick sequence of rhyolitic lavas, tuffs and perlitic-obsidian.

Dark red Low-velocity area which we assume as a hot spot **number 2** (Fig. 3) is approximately located on the northern slope of Aragats volcano (depth of ~7 to 13.66 km), which may be the reason for the existence of magma. Based on I.V. Chernyshev et al., 2002 and Vadim Milukov et al., 2018 studies, the Aragats center, one of the largest Quaternary volcanic centers in the Caucasus, is confined to the Aragats neovolcanic area located in the western part of Armenia, at the intersection of tectonic zones of a general Caucasian extension and the sublongitudinal Transcaucasus uplift. The development of the Pliocene-Quaternary volcanism of the Aragats area is defined by complex late collisional Geodynamics, which is related to global processes of the convergence of Eurasian and Arabian continental plates. The highest peak of the Lesser Caucasus, the polygene Aragats stratovolcano (altitude 4090 m, 70 km diameter), is situated in the western volcanic zone of the Aragats area which it occupies a special place in the neovolcanic evolution of Armenia in terms of diversity of the magmatic rocks, scales and duration of volcanism, variety of the eruption products, and intricacy of the geotectonic structure. The volcano represents a plan-convex asymmetric shield (40-42 km across) with a major crater in the northeastern part. The established duration of magmatic activity of the Aragats center is about 400 ka. Aragats volcano should presumably be ascribed to extinct volcanoes. Such large volcanoes (like Aragats), capable of generating many caldera collapse eruptions.

Dark red Low-velocity area which we assume as a hot spot **number 3** (Fig. 3) in our study covers a wide area such as Garni, Shoraghbyur, Yerevan, Avan salt dome and Harazdan from oil and gas resources introduced by Jrbashyan et al. (2001). The Paleocene and Lower Eocene of the subthrust section yielded oil-saturated cuttings and oil-cut mud and oil-stained cuttings were reported as features of the upper Eocene section in these area (thermogenic chemical interactions). By Milanovski, E.E., (1962) about this hot spot, detailed explanation is given as Sevan and Central Troughs. Due to the chemical interactions of in-earth materials in oil-rich areas (contains hydrocarbons) and gas resources, the temperature inside the earth is high and spots relevant with gas plumes is anomalously hot compared to the surrounding. The depth of this hot zone varies from 6.6 to 13.66 km.

Dark red Low-velocity area which we assume as a hot spot **number 4** (Fig. 3); is approximately located in the beneath of Ararat strato-volcanic structures (depth ~6.6-13.66 km, velocity 2 km/s) in the Julfa region, which could be due to the presence of a magma chamber beneath this volcanic complex. East-north foothills of this volcanic complex are affected by sediments of Aras river, which is limited by the uplifted basement of the Ararat volcanos to the south and by the Hrazdan Transverse Fault Zone to the west. Also, Ozgür Karaoğlu (2017) seismic tomography study indicates a magma reservoir at great depths (20-30 km) below the Ararat volcano. Geochemical constraints on some of the later-formed rocks suggest an interaction between a shallow chamber (8-10 km) and the deep reservoir approximately 0.5 Ma. This depth is consistent with the result of our study in period of 5 seconds (depth of 7-13 km; Fig. 3). Also, based on Jrbashyan et al., (2001) study, the Urts-Julfa Zone is limited by the uplifted basement of the Great Ararat to the south and by the Hrazdan Transverse Fault Zone to the west. Intersection with the Vedi Ophiolitic Belt is marked by a transition from alkali-basaltic volcanism to tholeiitic volcanism in the Mesozoic section. Relatively isolated strato-volcanic structures, such as Ararat and Aragats, occur at or near fault intersections. The largest volcanic edifice in this area is the Greater Ararat Stratovolcano, which

is composed of intermediate lavas with andesitic-dacitic-trachyandesitic compositions, erupted ~3.5 Ma (i.e. Piacenzian).

Dark red Low-velocity area which we assume as a hot spot **number 5** (Fig. 3) is approximately located in the northeast of the Lake Van includes Tendurek, Suphan and Nemrut Mountains. Study of Vural Oyan et al. (2018), shows collision related to Quaternary Mafic Volcanism to the north of Lake Van (Eastern Anatolia, Turkey) has been occurred by eruptions from both volcanic centers and extensional fissures trending approximately north-south. Also, the volcanic products in this area consist of mildly alkaline lavas and calculations based on crustal temperatures and Curie point depths indicate that the magma chamber might have been located at a depth of around 6-8 km, within the upper crust. We infer, that perhaps, the molten material beneath the Ararat volcano and the mountains around Lake Van are quite interconnected. In the period of 5 s in our study, this property has been shown at a depth of 6.6 to 13.66 km, which is consistent with Vural Oyan (2018) study. As well as, the pattern of concepts of hot spots 1, 4 and 5 is almost the same, as these regions are located in the Eastern Anatolia famous for its thin hot lithosphere structure.

Dark red Low-velocity area which we assume as a hot spot **number 6 and 7** (Fig. 3) are located in NW Iran near the north part of Sahand volcano and southeastern segment of the Tabriz fault. This fault is responsible destructive earthquakes in Tabriz (e.g. 7.7, 1721, Fig. 1). The epicenter of this earthquake, is located right into the hot zone number 6. It is clear that these hot spots are perhaps due to the interactions of the rocks of this famous active fault. Mehraj Aghazadeh et al. (2010) in a study has reported limited volcanic eruptions evidences in the South of the Tabriz fault (Sahand block) that are characterized by ages ranging from 11 Ma to present (era 4). The 11 Ma lavas have an alkaline potassic to ultrapotassic composition. Our results show distinct velocity anomalies for smaller periods along the North Tabriz Fault (NTF) and beneath the Sahand and Sabalan Volcanoes. In contrast, beneath the Sahand volcano a high-velocity zone is observed that could be due to the low temperature volcanic rocks or a deeper magma chamber at a depth of ~30.8 km.

Dark red Low-velocity area which we assume as a hot spot **number 8** (Fig. 3) is approximately located near a segment of Salvard fault in the north east of Nakhichevan. According to several studies (e.g. Danelian et al., 2014; Sokolov, 1977), exposures of Jurassic sequences are located in Nakhichevan and in Iran, where a 500 m -thick Lower and Middle Jurassic sedimentary sequence overlies Upper Triassic strata. Lower Cretaceous deposits are absent on the south Armenian block and the Triassic-Jurassic deposits are unconformably overlain by Cenomanian reefal limestones that are covered by marls. Upper Devonian (the fourth period of the Paleozoic era) and Permian (the fifth period of the Paleozoic era) rocks could be petroleum source rocks (Sosson et al., 2010). Silurian and Lower and Middle Devonian marine clastic and carbonate rocks crop out in Nakhichevan and are presumed to be present in Armenia. Our study is shown this property in period of 5 s at a depth of 6 to 9.5 km (hot spot number 8).

Dark red Low-velocity areas which we assume as a hot spots **number 9, 10, 11 and 12** (Fig. 3) in period of 10 s, in addition to the low-velocity anomalies during the period of 5 s, areas such as the eastern Black

Sea basin and a segment of the Odishi fault in the Rioni basin (number 9), the Nalchik city in Russia and north and south western of Kazbek mount (number 10), the Chatma region in east of Georgia (number 11) and South Caspian Basin (number 12) are also covered by low-velocity anomaly and it follows the same pattern described for the hot spots 1 to 8. As mentioned, the low-velocity anomaly beneath the volcanoes in the depth associated with this period (14 to 28.66 km), reveals the presence of magma and the magmatic reservoir and sediments.

Dark red Low-velocity area which we assume as a hot spots **number 13** (Fig. 3), the Elbrus volcanic complexes, Kazbek mount and Yanardag (natural gas fire on a hillside) in the great Caucasus have covered by the low-velocity anomaly. The low-velocity anomaly beneath the volcanoes in the depth associated (~30.8 km and 158.6 km) with these periods reveals the presence of magma and the magmatic reservoirs and mantle plume. In tomographic maps with long-period of 70 s (equivalent to a depth of 158.6 km); Azerbaijan, Kura and South Caspian basins and Talesh heights are covered with high-velocity, which we suggest cold lithosphere roots for deep areas. On the contrary, the low-velocity in the Greater Caucasus, eastern Black Sea basin and eastern Anatolia are resulting in very thin lithosphere and hot asthenosphere. The hot spots in period of 15 s follow the pattern described in periods of 5 and 10 seconds.

Dark red Low-velocity area which we assume as a hot spot **number 14** (Fig. 3) in periods of 40 and 45 seconds, is observed a wide hot spots area with low-velocity in the South Caspian Basin (SCB), below the Sahand-Sabalan volcanoes, Astara region, Tabriz Fault and slightly in the southernmost mountain around Lake Van or Bitlis Massif in the border of Iraq, which, according to (Sugden et al., 2018) study, the mid-lithosphere magma source has a distinct composition compared to the base of the lithosphere, that is argued to be the result of the increased retention of metasomatic components in phases such as apatite and amphibole, that are stabilized by lower temperatures prior to magma generation. Also, partial melts of the deep lithosphere ~120 km (in our study 111 km) and mid-lithosphere sources to give a composition intermediate between magmas from the northern Lesser Caucasus and NW Iran could be the reason for this extensive hot spot.

Dark red Low-velocity area which we assume as a hot spot **number 15** (Fig. 3) in the period of 45 and 50 seconds, is observed a wide very low-velocity anomaly in east and northeast of Lake Van and just east of the Ararat, Sahand, Sabalan, Bitlis, Nakhchivan, South Armenia, Astara, South Caspian Basin. According to some studies (e.g. Kearey, Philip et al. 2009; Condie, Kent C., 1997); this decrease of seismic wave velocity from lithosphere to asthenosphere, could be caused by the presence of a very small percentage of melt in the asthenosphere and seismic waves pass through the lithosphere-asthenosphere very slowly. Also, the lower boundary of the LVZ lies at a depth of 180-220 km (our study ~175 km), therefore, the hot wide area is not unexpected. We propose that perhaps it marks the depth of LAB and LVZ in Caucasus region and so the wave has penetrated to the asthenosphere layer and seismic waves pass through this area very slowly. The interactions and intrusion of very hot molten material from asthenosphere to lithosphere discontinuities for creating hot spot number 15 is not unexpected. Fig. S6 of the Supplementary Materials has been depicted the approximate depth of Moho, LAB and LVZ for this study.

In the Lesser Caucasus, there is the link between the volcanic manifestations and low-velocity patterns, but it is not as clear as in the Great Caucasus. The Gegham volcanic group in Armenia also match with the location of the low velocity anomaly. Also, in Sugden et al. (2018) study, diagram of depth vs temperature of melting shows that after the depth of 150 km, the temperature has a significant increase in Gegham, Syunik, and Vardenis.

Long-period tomographic maps velocity structures of 55 to 70 (approximate depth of 200 km), indicate ultrahigh-velocity anomalies (5.04 km/s) and ultralow-velocity (1.4 km/s) areas. We infer the deep ultrahigh-velocity anomalies may be the broken off cold lithosphere generated slabs were sinking into the mantle transition zone and very-hot upper mantle with low mantle lid (cap). In contrast, for ultralow-velocity regions, is thought that the upper mantle has been rejuvenated by a phase of the upwelling hot mantle, and this metasomatic refertilization of the upper Cratonic mantle has increased its density and reduces seismic velocity and rocks experience temperatures above 1300-1600 ℃ at these depths. Also, according to depth-temperature diagrams (e.g. Sugden et al. 2018), at these depths, some interactions such as onset of dry melting in the convecting mantle and the Spinel out or hard-glassy mineral occurring as octahedral crystals of variable color and consisting chiefly of magnesium and aluminum oxides, cause an increase in temperature and density conflicts tension. So, we propose that at the depths common between the lithosphere-asthenosphere-upper mantle; anomalies accumulation, inhomogeneities and antagonistic behaviors are common in surface wave velocity variations. In these regions, due to continuous changes in temperature caused by the plate tectonic activity, the effect of active liquids penetrated by the asthenosphere, subsidence, uplifts, hot asthenospheric diapirs intrusion, the velocity of surface waves changes. Also, seismic waves slowly cross the lithosphere-asthenosphere boundary (LAB), which known as the low-velocity zone (LVZ), and then enter the upper mantle (Fig. S6). Poor coverage of ray paths in this part of the study area (periods of 60, 65 and 70 s) leads to stretching and smearing (butterfly-shaped areas) by this feature toward the northwest and southeast of the study area. In these periods, due to some reasons such as plates tectonic activities, hot asthenospheric diapirs intrusion, the effect of active liquids penetrated by the asthenosphere, subsidence, uplifts and mantle plumes the temperature changes constantly and therefore, the surface waves have variable behavior.

5. Discussion

Hot spots and related structures in the mantle to understand the dynamics of Earth and the modes of heat transfer inside the planet is very important and there are evidences for subduction or underplating crust in those regions. In here, we're looking for cold and hot spots inside the Earth. Therefore, using the tomography technique and increasing-decreasing the surface wave velocity anomalies in different areas of the study area, were determined hot and cold spots. In other words, according to the seismic tomography images results from within the earth, we are looking for the following results in the period of 5 to 70 seconds: 1. Dark blue shades mean colder and stiffer rock (Cold Spots- areas with fast wave velocity) 2. Dark red shades mean warmer and weaker regions (Hot Spots- areas with slow wave velocity) 3. Green-blue-yellow color, are the remnants of an old tectonic plate that has been subducted underneath the Earth's plates (large cold and aseismic area during million years). So, our tomography maps show the

hotter regions with dark red color where there are diapirs intrusion, mantle plumes, chain of volcanoes, and fault activity. And the maps with dark blue-green-yellow color shows the colder regions where oceanic plates have sunk into earth's interior in the past, supporting the idea that dense slabs of oceanic crust may penetrate to the lower mantle (underlie areas).

Short periods of 5 to 20 seconds include the most number of hot-cold spots in the study area and approximately 13 major hot spots with a depth of 6.6 to 30.8 km with velocity of 1.4 to 2 km/s were identified for different geological units of the region. The location of these hot-cold spots are in good agreement with the results of mentioned tomographic studies in this region. Since the geothermal resources are shallow-crustal phenomena (uppermost few km of the crust), so these short-period hot spots, are located in an appropriate depth of shallow area of the earth's crust as geothermal energy for humans. In fact, this is the first study to determine and interpret the hot-cold spots of the Caucasus region using Rayleigh surface wave velocity, and so far, no study has been conducted that directly examines the hot-cold spots in the Caucasus using decreasing and increasing the surface wave velocity. As well as, determined hot spot and cold spot (15 regions) follows physical processes within the earth and magma generation in Fig. S7 steps. Based on tomographic maps in periods of 5 to 70 seconds and geological evidences, 15 hot spots with dark red shades in the study area were determined and analyzed and the rest of the areas with dark blue-green-yellow shades are cold spots, which represents the remnants of an old tectonic plate that has sunk beneath the Earth's plates. Furthermore, tomographic maps with distinct velocities over short-periods of 5 to 25 seconds (equivalent to a depth of 6 to 53 km), are more sensitive to the structure of the upper to lower crust and Moho. These periods represent sediments in the basins, chemical interactions of hydrocarbon resources, molten material, magma chambers beneath volcanoes and Moho discontinuity which these areas can be considered *temporary* and *unstable* hot-cold spots. In tomographic maps with medium-periods of 30 to 50 seconds (equivalent to a depth of 68 to 167 km), Azerbaijan, Kura and South Caspian basins and Talesh heights are covered with high-velocity, which we propose cold lithosphere roots for these areas. On the contrary, are observed the low-velocity in the east of the Greater Caucasus, Eastern Black Sea Basin, Eastern Anatolia and NW Iran, resulting in very thin lithosphere and hot asthenosphere in the region which these areas can be considered *temporary* and *semi-stable* hot-cold spots. Long-period tomographic maps velocity structures of 55 to 70 s (depth of ~200 km), show that ultrahigh-velocity anomalies have been spread under the South Caspian Sea Basin, Kura Basin, Baku, NW Iran and Bitlis Massif; while a wide area is covered with ultralow-velocity. We interpret the deep ultrahigh-velocity anomalies may be the broken off cold lithosphere generated slabs were sinking into the mantle transition zone and very-hot upper mantle with low mantle lid (cap). Also, high-velocity in the eastern Greater Caucasus and South Caspian Sea Basin is a part of the ongoing subduction system and asthenosphere with significant amounts of melt is the major factor producing this ultralow-velocity zone in the region which these areas can be considered *permanent* and *stable* hot spots.

6. Conclusions

In this study, we have performed the first 2D tomography maps of Rayleigh wave for the entire Caucasus using developed method by Yanovskaya-Ditmar. The derived 2D tomography velocity anomaly maps of Rayleigh wave dispersion curves, were carefully verified using fundamental mod of vertical (Z) component of earthquake waveform energy in order to identify hot-cold spots, understand better the regional tectonic activities, faults activities and lithospheric blocks interactions as geothermal resources and surface waves velocity variations in the ongoing collision-compressed edge zone of the Eurasian-Arabic plates. These maps show excellent agreement with many of the geological features of the Caucasus territory, such as Volcanoes Complex, Troughs, Uplifts and Basins. Also, 15 low-velocity area (hot spots) were identified that the Hot Spots Number 10, 11 and 13 (in Greater Caucasus); Number 1, 4 and 5 (Eastern Anatolia); Number 2, 3 and 15 (Lesser Caucasus-Armenia); Number 6, 7 and 14 (NW Iran); Number 12 in the South Caspian Sea Basin; Number 9 (Rioni-Eastern Black Sea Basin) and Number 8 are located NW of Nakhchivan and is in good agreement with previous studies and geological evidence. The rest of the areas with dark blue-green-yellow shades are cold spots, which represents the remnants of an old tectonic plate that has sunk beneath the Earth's plates. The hot spots close to the earth's surface (beneath our feet) during the short periods can be considered as geothermal resources to provide the heat energy of cities and power plants (e.g. hydrothermal of Sabalan volcano in Iran-Ardabil and Iceland-Nesjavellir Geothermal Power Plant).

Declarations

Acknowledgments

Thanks to the Iranian Seismological Center, Incorporated Research Institutions for Seismology (IRIS) Data Management Centre, Iranian National Seismological Network, National Strong-Motion Network of Turkey (TR-NSMN), National Seismic Network of Turkey (DDA), National Seismic Network of Azerbaijan and National Seismic Network of Georgia who provided some of the seismic data used in this study. Many of the figures in this paper were prepared using GMT (Wessel & Smith 1995), which thank them. We also thank the Institute of Geophysics of the University of Tehran, which managed and supported this study in the framework of the educational mission (2016-2018).

Author contributions

S.H.A. designed research, gathered, prepared and analyzed data and wrote and executed computer code under the supervision of H.R. and J.K.K. and E.G. are also supervisor and advisor of the study. All authors contributed to discussions and interpretation of geological-geodynamic of the region and S.H.A. after final discussions with H.R., J.K.K. and E.G. wrote the paper.

Competing interests

The authors declare no competing interests.

References

1. Ryan, C., Porter, van der Lee & Steven, J. Suzan & Whitmeyer Synthesizing EarthScope data to constrain the thermal evolution of the continental U.S. lithosphere, Geosphere (2019) 15 (6): 1722–1737, https://doi.org/10.1130/GES02000.1 (2019)
2. Wilson, J. & Tuzo A possible origin of the Hawaiian Islands. *Canadian Journal of Physics*, https://doi.org/doi:10.1139/p63-094 (1963).
3. Michael Wysession Unlocking the secret of the North American continent, an EarthScope science plan, http://epsc.wustl.edu/seismology/michael/web/activities.html (2010-2020)
4. Ditmar, P. G. & Yanovskaya, T. B. Generalization of Backus-Gilbert method for estimation of lateral variations of surface wave velocities. *Phys. Solid Earth, Izvestia Acad. Sci. USSR*, **23** (6), 470–477 (1987).
5. Yanovskaya, T. B. & Ditmar, P. G. Smoothness criteria in surface wave tomography. *Geophys. J. Int*, **102**, 63–72 (1990).
6. Gheitanchi, M. R. Crustal structure in Nw in Iran, revealed from the 1990 Rudbar aftershock sequence. *J. Earth Space Phys*, **23**, 7–14 (1996).
7. Skobeltsyn, G. *et al.* Upper mantle S wave velocity structure of the East Anatolian-Caucasus region, Tectonics, 33,207–221, doi:10.1002/2013TC003334, (2014)
8. Randolph, J. *et al. Caucasus Seismic Information Network: Data and Analysis* (New England Research, Inc, 2007).
9. Golonka, J. Plate tectonic evolution of the southern margin of Eurasia in the Mesozoic and Cenozoic., **381**, 235–273 (2004).
10. Hatzfeld, D. & Molnar, P. Comparisons of the kinematics and deep structures of the Zagros and Himalaya and of the Iranian and Tibetan Plateaus and geodynamics implications, Rev. Geophysics., 48, RG 2005, doi:10.1029/2009RG000304 (2010)
11. Copley, A. & Jackson, J. Active tectonics of the Turkish-Iranian Plateau, Tectonics, 25, TC6006 (2006)
12. Jackson, J. Partitioning of strike-slip and convergent mountain between Eurasia and Arabian in Eastern Turkey and the Caucasus. *J. Geophys. Res*, **97**, 12471–12479 (1992).
13. Talebian, M. & James, J. Offset on the Main Recent Fault of NW Iran and implications for the late Cenozoic tectonics of the Arabic-Eurasia collision zone. *Geophys. J. Int*, **150**, 422–439 (2002).
14. Bavali, K. *et al.* Lithospheric structure beneath NW Iran using regional and teleseismic travel-time tomography. *Physics of the Earth and Planetary Interiors*, **253**, 97–107 (2016).
15. Simon *et al.* Global Positioning System constraints on plate kinematics and dynamics in the eastern Mediterranean and Caucasus, DOI: 10.1029/1996JB900351(2000)
16. Sosson, M., Stephenson, R. & Adamia, S. Tectonic Evolution of the Eastern Black Sea and Caucasus, https://doi.org/10.1144/SP428.16 (1977)
17. Alik Ismail-Zadeh Geodynamics, seismicity, and seismic hazards of the Caucasus, https://doi.org/10.1016/j.earscirev.2020.103222 (2020)

18. Jrbashyan, R. *et al. Geology of Meso-Cenozoic Basins in Central Armenia* (with Comment on Indications of Hydrocarbons, 2001).
19. Khuduzade, A. I. *et al.* Structural-tectonic features of the south-eastern part of the Greater Caucasus the pre-Caspian GUBA as an example of the NQR(2017)
20. Herrmann, R. B. & Ammon, C. J. Computer Programs in Seismology, 3.30[CP/OL]. http://www.eas.slu.edu/eqc/eqccps. Html (2004)
21. Shota *et al.* Geology of the Caucasus: A Review(2011)
22. Kinahan, P. & Townsend, D. Attenuation correction for a combined 3D PET/CT scanner, Med Phys., (1998)
23. Backus, G. E. & Gilbert, F. The resolving power of gross earth data. *Geophys. J*, **16**, 169–205 (1968).
24. Lihua, F. *et al.* Rayleigh wave tomography in North-China from ambient seismic noise(2008)
25. Duru *et al.* Magmatic Evolution of the ALADAĞ Volcanic System and Southern Edge of the Erzurum-Kars Volcanic Plateau (SARIKAMIŞ, City of Kars, NE Turkey), Bibcode: 2020 EGUGA. 2221626D(2020)
26. Sengör, A. M. C. *et al.* East Anatolian high plateau as a mantle supported, north-south shortened domal structure. *Geophys. Res. Lett*, **30**, 8045 https://doi.org/doi:10.1029/2003GL017858 (2003).
27. Chernyshev, I. V., Lebedev, V. A. & Bubnov, S. N. M.M. Arakelyants Isotopic geochronology of Quaternary volcanic eruptions in the Greater Caucasus (2002)
28. Vadim *et al.* Contemporary State of the Elbrus Volcanic Center (The Northern Caucasus), DOI: 10.1007/s00024-017-1595-x (2018)
29. Milanovski, E. E. Sevan Basin. In: Geology of Armenian SSR, v. 1, Geomorphology, Ar. Ac. Sci. Publ., Yerevan, 1962, p. 115-136 (in Russian) (1962)
30. Ozgür, K. Ä. *et al.* Volume lava flows fed by a deep magmatic reservoir at Ağrı Dağı (Ararat) volcano, Eastern Turkey, DOI: 10.1007/s00445-016-1098-0 (2017)
31. Vural Oyan Geochemical and petrologic evolution of Otlakbaşı basaltic volcanism to the east of Lake Van, DOI: 10.19111/bulletinofmre.427782 (2018)
32. Mehraj *et al.* The gabbro (shoshonitic)-monzonite-granodiorite association of Khankandi pluton, Alborz Mountains, NW Iran, DOI: 10.1016/j.jseaes.2010.01.002 (2010)
33. Danelian, T. *et al.* Reconstructing Upper Cretaceous paleoenvironments in Armenia based on Radiolaria and benthic Foraminifera, http://dx.doi.org/.10.1016/j.palaeo. 2014.03.011 (2014)
34. Sokolov, S. D. *The Olistostromes and Ophiolitic Nappes of the Lesser Caucasus* (Izdatelstvo 'Nauka', Moscow, 1977). (in Russian)
35. Sosson, M. *et al.* Sedimentary Basin Tectonics from the Black Sea and Caucasus to the Arabian Platform, http://dx.doi.org/10.1144/SP340.14 0305-8719/10 (2010)
36. Sugden, P. J. *et al.* The Thickness of the Mantle Lithosphere and Collision-Related Volcanism in the Lesser Caucasus(2018)
37. Kearey, P. *et al.* Global tectonics(2009)

38. Condie, K. C. Mantle plumes and their record in Earth history (2001)

Figures

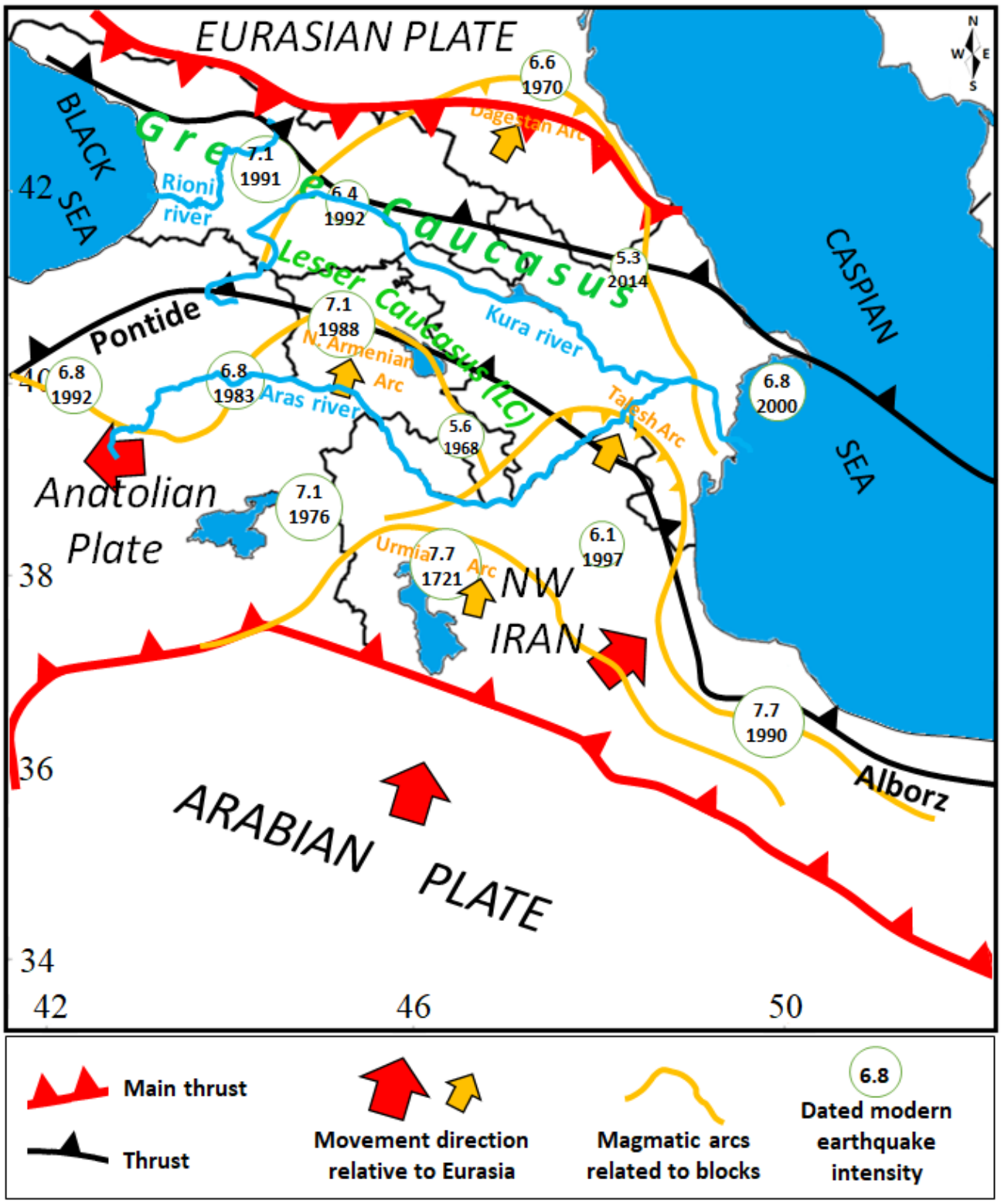

Figure 1

Active tectonic features of the collision zone of the Central Eurasian- Arabian. The arcs are retrieved from Jrbashyan et al. (2001). The main thrusts are retrieved from A.I. Khuduzade, et al. (2017).

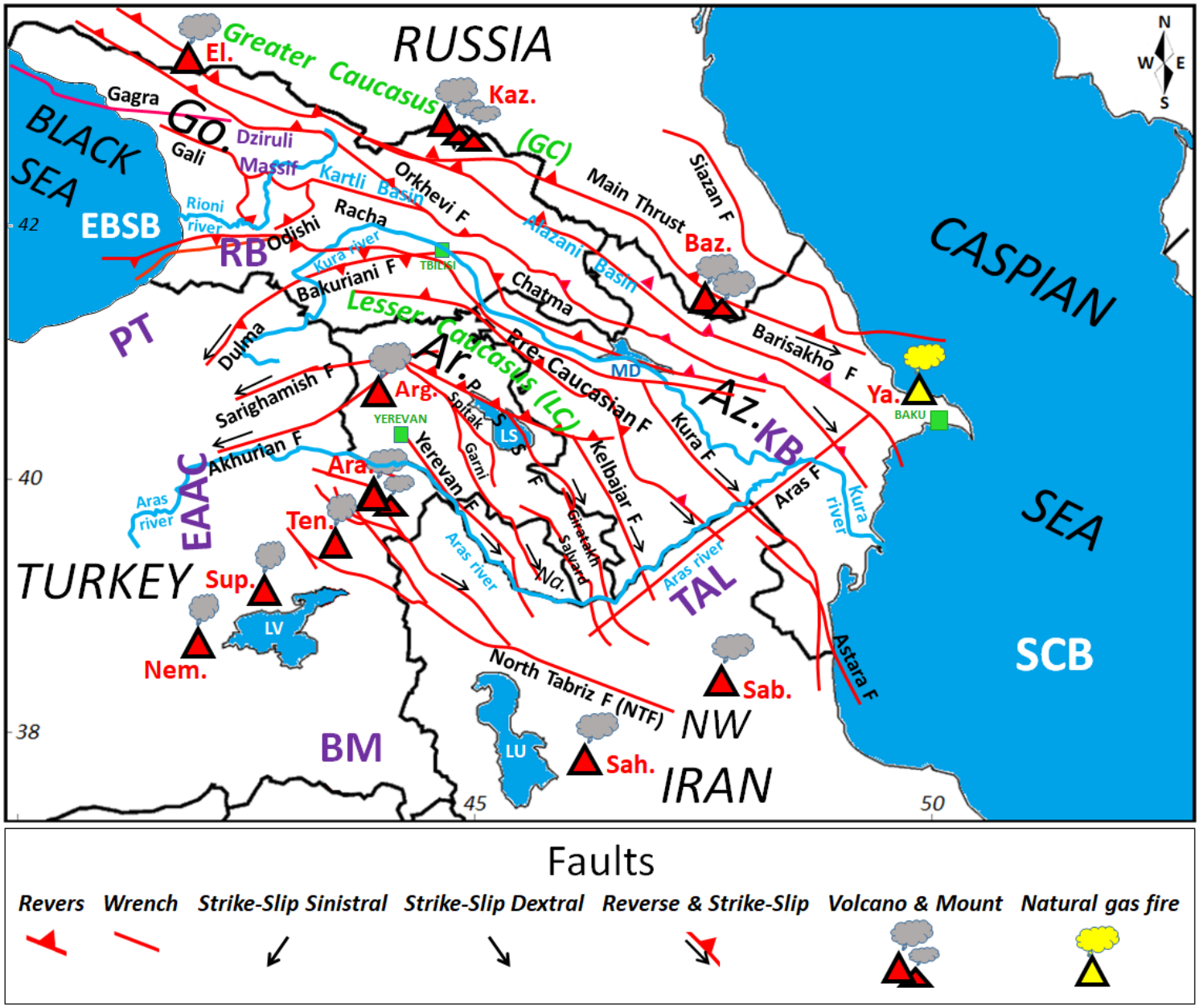

Figure 2

Geological units discussed in the interpretation of 2D tomography maps, faults, volcanoes, rivers and basins in the study area. Abbreviations: F= Fault, Sab.= Sabalan, Sah.= Sahand, Nem.= Namrout, Sup.= Suphan, Ten.= Tendourek, Ara.= Ararat, PT= Pontide, BM= Bitlis Massif, EAAC= East Anatolian Accretionary Complex, Arg.= Aragats, El.= Elbrus, Kaz.= Kazbek, Baz.= Bazarduzu mount, Ya.= Yanardag (natural gas fire on a hillside), Na.= Nakhchivan, Go.= Georgia, Ar.= Armenia, Az.= Azerbaijan, LV= Lake Van, LU= Lake Urmia, LS= Lake Sevan, MD= Mingachevir Dam, TAL= Talesh, KB= Kura Basin, RB = Rioni

Basin, SCB= South Caspian Basin, EBSB= Eastern Blake Sea Basin, PSSF= Pambak-Sevan-Syunik Fault. The seismic sources (faults) of the Caucasus are retrieved from Shota Adamia et al. (2011).

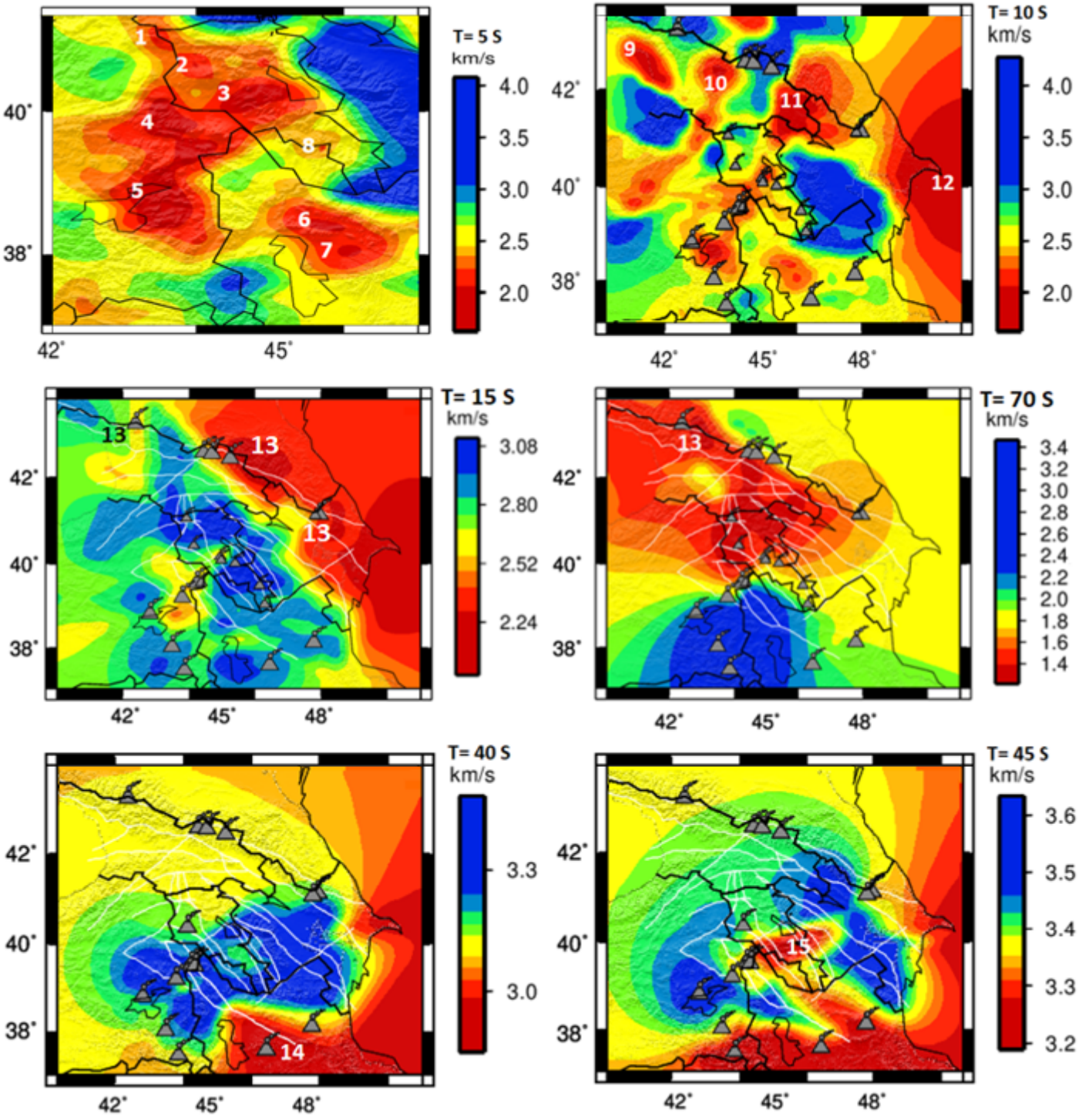

Figure 3

Labeled areas number 1 to 15 are the major low-velocity with dark red shade (slow) that we assume as hot spots and the rest of the areas with dark blue-green-yellow shades are high-velocity (fast) cold spots,

which represents the remnants of an old tectonic plate that has sunk beneath the Earth's plates in our study. Greater Caucasus hot spots are shown with the number 13. The white lines are faults and the gray triangles are volcanoes and mount.

Supplementary Files

This is a list of supplementary files associated with this preprint. Click to download.

- SupplementaryTheCaucasusTerritoryHotColdSpotsDeterm.pdf